Mon. Not. R. astr. Soc. (1985) **213,** 613–639

The galactic population of pulsars

A. G. Lyne *University of Manchester, Nuffield Radio Astronomy Laboratories, Jodrell Bank, Macclesfield, Cheshire SK11 9DL*

R. N. Manchester *Division of Radiophysics, CSIRO, PO Box 76, Epping, NSW 2121, Australia*

J. H. Taylor *Joseph Henry Laboratories, Princeton University, and Institute for Advanced Study, Princeton, New Jersey 08544, USA*

Accepted 1984 November 9. Received 1984 November 8; in original form 1984 August 14

Summary. In order to draw statistical conclusions about the overall population of pulsars in the Galaxy, we have analysed a sample of 316 pulsars detected in surveys carried out at Jodrell Bank, Arecibo, Molonglo, and Green Bank. We quantify the important selection effects of each survey, and describe a statistically reliable pulsar distance scale based on a model for the large-scale distribution of free electrons in the Galaxy. The distance scale is calibrated by independent distance estimates for 38 pulsars. These results allow the spatial and luminosity distribution functions of galactic pulsars to be computed. We conclude that the Galaxy contains approximately 70 000 potentially observable pulsars with luminosities above 0.3 mJy kpc^2. Most of these pulsars have luminosities less than 10 mJy kpc^2, more than an order of magnitude less than the mean luminosity of the observed sample. The distribution in galactocentric radius rises smoothly through the solar location towards the galactic centre and peaks inside 6 kpc, again in contrast to the observed sample which peaks near the Sun. The galactic z distribution has a scale height of about 400 pc, much larger than that of the OB stars from which pulsars form.

We then consider the period and luminosity evolution of pulsars, using an approach similar to that developed by Gunn & Ostriker, and show that the observed distributions of period, period derivative and galactic z distance can be accounted for without invoking either late turn-up or an abrupt cut-off in the pulsed luminosity. The derived time constant for decay of the magnetic field is approximately 9 Myr. The pulsar birthrate required to maintain the observed population is one every 30 to 120 yr – in satisfactory agreement with the galactic supernova rate, the birthrate of supernova remnants, and the death rates of stars in the mass range generally thought to leave neutron star remnants.

1 Introduction

There are now approximately 370 known pulsars, and studies of their luminosity function and their distribution in space indicate that the total number in the Galaxy is at least one hundred times larger. Because the observed sample is such a small fraction of the whole, statistical conclusions regarding characteristics of the entire population must be drawn with care. In particular, the observational selection effects involved in pulsar surveys must be evaluated quantitatively and then used to convert the measured sample observables into parameters of the much larger parent population.

Early efforts along these lines were made by Gunn & Ostriker (1970) and by Large (1971). At that time only a few dozen pulsars were known, and period derivatives had been measured for less than half of them, so statistical uncertainties were large. Furthermore, pulsar searching techniques were varied and somewhat haphazard, selection effects were hard to quantify, and a reliable distance scale for pulsars was unavailable. Attempts to discover characteristics of the pulsar population as a whole were therefore plagued with large systematic uncertainties.

In the next few years, extensive pulsar surveys were carried out at the Jodrell Bank and Arecibo observatories (Davies, Lyne & Seiradakis 1972, 1973; Hulse & Taylor 1974, 1975), and many additional period derivatives were measured (Manchester & Peters 1972; Lyne, Ritchings & Smith 1975), so much more thorough studies of the galactic distribution and evolution of pulsars could be made. By 1976 nearly 150 pulsars had been found, and 85 period derivatives measured. In addition, measurements of neutral hydrogen absorption at $\lambda 21$ cm had provided distance estimates for a number of pulsars (Graham *et al.* 1974; Gomez-Gonzalez & Guelin 1974; Gordon & Gordon 1975; Ables & Manchester 1976; Booth & Lyne 1976). Armed with this information, Davies, Lyne & Seiradakis (1977) and Taylor & Manchester (1977) independently reached the conclusion that the Galaxy presently contains at least 10^5 active pulsars, and that the pulsar birthrate may be as large as one every three to 40 years.

Not long after these papers were published, two more pulsar surveys were completed: the second Molonglo survey, covering most of the sky south of declination +21° (Manchester *et al.* 1978) and the University of Massachusetts–National Radio Astronomy Observatory survey, covering about two thirds of the northern sky to approximately the same sensitivity limit (Damashek, Taylor & Hulse 1978; Damashek *et al.* 1982). These efforts again more than doubled the number of known pulsars, and follow-up observing programmes succeeded in measuring period derivatives for most of them (Gullahorn & Rankin 1978; Newton, Manchester & Cooke 1981; Ashworth & Lyne 1981; Backus, Taylor & Damashek 1982). Thus, the entire sky has now been surveyed to a reasonably well calibrated flux density limit, with well-understood dependences of sensitivity on period, dispersion measure and direction in the sky. Furthermore, measurements of flux densities, periods and period derivatives are now available for nearly all the known pulsars.

For the first time, therefore, it is possible to analyse a large, statistically significant sample of pulsars with well-understood instrumental selection effects and without strong observational bias as to direction in the sky. Papers written recently presenting various analyses of the data include those by Gailly, Lequeux & Masnou (1978), Arnaud & Rothenflug (1980), Fujimura & Kennel (1980), Huang *et al.* (1980), Arnett & Lerche (1981), Phinney & Blandford (1981), Morini (1981), Vivekanand & Narayan (1981), Guseinov, Kasumov & Yusifov (1982b), Harding & Harding (1982), Vivekanand, Narayan & Radhakrishnan (1982). In general, however, we believe that these papers have not adequately accounted for selection effects in the surveys, nor adopted a satisfactory model for the evolution of pulsar luminosities, nor made good use generally of the valuable kinematic information provided by pulsar motion studies (Manchester, Taylor & Van 1974; Anderson, Lyne & Peckham 1975; Backer & Sramek 1981; and especially Lyne, Anderson & Salter 1982).

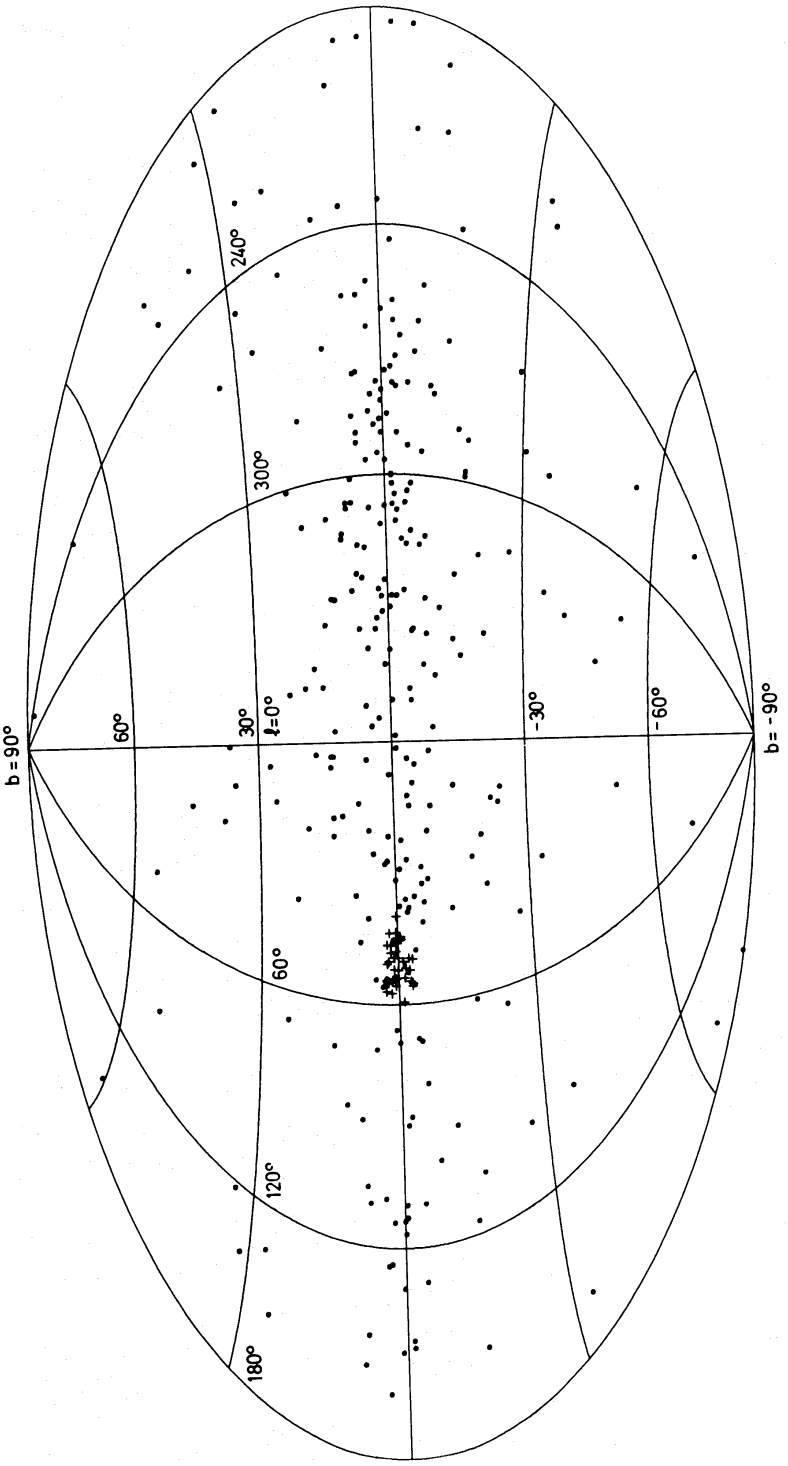

Figure 1. Distribution in galactic coordinates of the 316 pulsars detected in the Jodrell Bank, second Molonglo, and UMass–NRAO surveys (dots) and in the UMass–Arecibo survey (crosses).

Our aim in the present paper, then, is to rectify these deficiencies and to take a fresh look at the galactic population of pulsars. Our basic observational sample consists of all pulsars observed in the Jodrell Bank, Arecibo, second Molonglo, and UMass–NRAO surveys, a total of 316 pulsars. Except for the Arecibo survey, which was nearly an order of magnitude more sensitive, each survey could detect a minimum pulsar flux density of about 10 mJy at 400 MHz, at least for pulsar periods greater than about 200 ms. Thus, excepting the Arecibo pulsars, our list represents an approximately flux-limited sample. The distribution of the sample pulsars in galactic coordinates is shown in Fig. 1.

The plan of our paper is as follows. In Section 2, we discuss the present state of affairs in measuring pulsar distances; a sound basis for estimating individual pulsar distances and their uncertainties is essential to many arguments in the rest of the paper. In Section 3 and Appendices A and B we quantify the important selection effects in each of the four surveys, and then calculate the intrinsic distribution functions that describe the number density of pulsars with respect to galactocentric radius R, distance from the galactic plane z, and luminosity L. Section 4 then treats the question of luminosity evolution and derives the birthrate required to maintain the observed galactic population of pulsars. We discuss some implications of our results and summarize our conclusions in Section 5.

2 The pulsar distance scale

Before we can estimate the spatial density and birthrate of pulsars in the Galaxy, distances to the observed pulsars must be known. For most pulsars the dispersion measure, together with a model for the galactic electron density distribution, provides the only available indicator of distance. Unfortunately, there is no way of independently estimating the interstellar electron density to sufficient accuracy, so the pulsars themselves must be used to calibrate the distance scale in bootstrap fashion.

There are currently three ways of obtaining distance estimates for pulsars independent of dispersion measurements: from association of the pulsar with a supernova remnant, from interferometric measurements of annual parallax, and from neutral hydrogen absorption measurements together with a galactic rotation model. Pulsar–supernova associations have been established convincingly for only three pulsars – PSR 0531+21 (the Crab Nebula), PSR 0833−45 (the Vela supernova remnant), and PSR 1509−58 (G320.4−1.2) (see Manchester & Taylor 1977; Manchester, Tuohy & D'Amico 1982.) Significant measurements of annual parallax have been obtained for two pulsars, PSR 0950+08 and PSR 1929+10 (Salter, Lyne & Anderson 1979; Backer & Sramek 1981; Taylor *et al.* 1984). Estimates of pulsar distances from H I absorption data have been obtained for a total of 33 pulsars and are summarized (with references to the original literature) by Manchester & Taylor (1981).

With the exceptions noted below, we have adopted the distances quoted by Manchester & Taylor (1981) as a basis for calibrating the distance scale. Recent measurements of H I absorption using the 64-m telescope at Parkes (*cf.* Manchester, Wellington & McCulloch 1981) have provided improved estimates of distance for two pulsars, PSR 1054−62 (12–20 kpc) and PSR 1240−64 (4–6 kpc) and these new values are used in preference to the values quoted by Manchester & Taylor (1981). For PSR 1509−58 we adopt the distance of 4.2 kpc given by Caswell *et al.* (1975) for the associated supernova remnant G320.4−1.2 and for PSR 0950+08 we adopt the value 0.13 kpc obtained from annual parallax measurements (Taylor *et al.* 1984).

The galactic electron density model that we find to be most consistent with the independently determined pulsar distances, while requiring a minimum of adjustable parameters or *ad hoc* assumptions, consists of three components: a layer of much greater scale height than that of the pulsars themselves, approximated by a constant density of 0.025 electron cm^{-3}; a thin layer, of

density 0.015 cm^{-3} on the galactic plane and scale height 70 pc, which statistically represents the contributions of the ionized regions surrounding hot population I stars and clusters; and a third component which explicitly models the electron content of the Gum Nebula. For reasons described below, the first two terms are also given a weak dependence on galactocentric radius, R. The model is defined by the equation

$$n_e=\left[0.025+0.015\exp\left(-\frac{|z|}{70}\right)\right]\left[\frac{2}{1+R/10}\right]+0.28\,\alpha_{GN}, \tag{2.1}$$

where n_e is in cm^{-3}, the distance from the galactic plane z is in pc, the galactocentric radius R is in kpc, and α_{GN} is unity within and zero outside the physical boundaries of the Gum Nebula. (The Sun is assumed to be at $R=10$ kpc, $z=0$.) Except where an independent distance estimate was available, the model distance to each pulsar was computed by integrating the electron density along the line-of-sight until the observed dispersion measure was reached.

The constants in equation (2.1) were evaluated in the following manner. First, we modelled the contribution from Galactic H II regions by considering the ionizing stars and clusters within a kiloparsec of the Sun, as listed by Prentice & ter Haar (1969). The radius of each of the nearby H II regions was recomputed using the ionizing fluxes given by Richstone & Davidson (1972), together with a mean interstellar gas density of 1 cm^{-3}. (For H II regions that are visible on the wide angle Hα photographs by Sivan (1974), the observed radius was used instead, and the gas density adjusted to be consistent with the ionizing flux.) We found that, if they were smoothed out over space, the electrons in the nearby H II regions would be adequately modelled by the function

$$n_e=0.015\exp\left(-\frac{|z|}{70}\right). \tag{2.2}$$

The scale height of 70 pc is comparable to that for extreme population I material (e.g. Georgelin & Georgelin 1976).

The Gum Nebula is exceptional in the present context because it is large and close, and extends to high latitudes. Therefore an explicit dispersion measure contribution for this H II region, represented by the last term in equation (2.1), was added to our model. The parameters we assumed for the nebula are: galactic coordinates $l=260°$, $b=0°$, distance=500 pc, radius=115 pc, and $n_e=0.28\,cm^{-3}$.

The value of the first constant in equation (2.1), which quantifies the large scale-height component of the electron distribution, was determined by requiring that for all pulsars having independent distance estimates, the sum of the model distances be equal to the sum of the independent distances. The computed value for the coefficient was very close to 0.025 cm^{-3}, so this rounded value was adopted.

We performed a number of tests to check the validity of the adopted electron density model. Following Hall (1980), we arranged the list of pulsars having independent distance estimates in order of increasing $|z|=d\sin|b|$, and then computed

$$\langle n_e\rangle=\sum DM\Big/\sum d \tag{2.3}$$

where DM is dispersion measure and d is distance, for contiguous groups within the ordered list. Unlike Hall, we did not include pulsars with only a single bound on the distance, in order to avoid a bias in the results caused by a few unrealistic values for these bounds. This approach left us with a total of 23 pulsars grouped in five groups of four and one of three. The fit of the dominant terms of our model,

$$0.025+0.015\exp\left(-\frac{|z|}{70}\right),$$

to these data is comparable to the fit of Hall's model, characterized by

$$n_e = 0.048 \exp\left(-\frac{|z|}{264}\right). \tag{2.4}$$

In a second test, our adopted model proves to be clearly superior to the Hall model. Distances to known pulsars were computed from the observed dispersion measures according to our model, the Hall model, and a simple model with constant electron density $n_e = 0.03\,\mathrm{cm}^{-3}$ everywhere. The pulsars were arranged according to distance from the Sun in 1 kpc bins, and the average distance of pulsars from the galactic plane, $\langle |z| \rangle$, was computed for each bin. The results are plotted in Fig. 2. Since the solar location is not special in galactic terms, and since the z-dispersion of pulsars is dominated by kinematic effects (Lyne *et al.* 1982), we expect $\langle |z| \rangle$ to be essentially independent of distance. The Hall model clearly fails this test, evidently because it

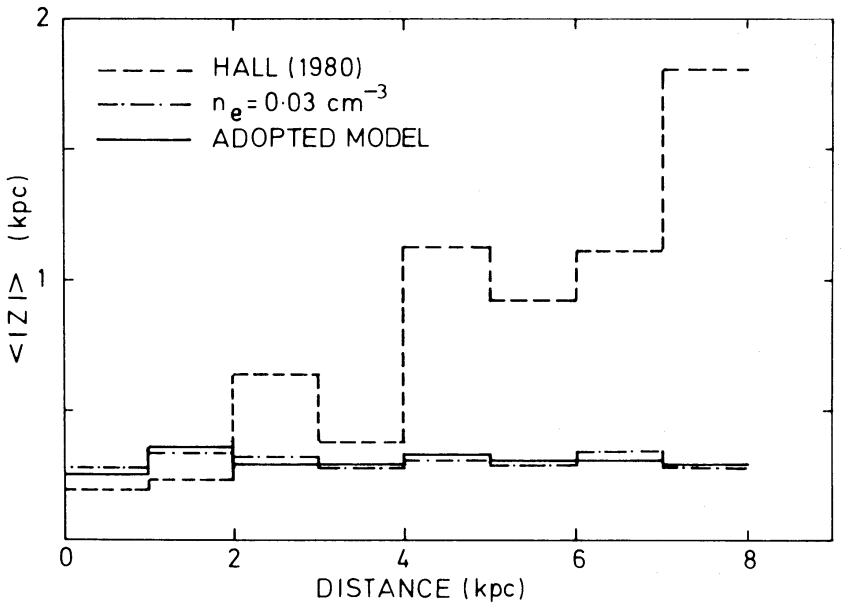

Figure 2. Mean $|z|$ for pulsars plotted as a function of distance from the Sun, with distances computed from three different models of interstellar electron density.

overestimates the distances of most high dispersion pulsars. The constant-density model, on the other hand, is as good as the adopted model with respect to this test.

A third test was applied in which $\langle |z| \rangle$ for the derived galactic pulsar distribution, that is, the distribution after correction for observational selection efects, as discussed in Section 3, was plotted against galactocentric radius R. The weak R-dependence in our model (equation 2.1) was chosen empirically to flatten the resulting graph of $\langle |z| \rangle$ versus R.

As an indication of the reliability of our model for computing pulsar distances, Fig. 3 presents a plot of independently derived distances versus model distances. Of the 38 pulsars plotted, all but five have measured distances or limits within a factor of two of the model distance, and all of these five are nearby objects, $\lesssim$1 kpc from the Sun. In these cases the discrepancies probably arise as a result of electron density fluctuations on scales of $\lesssim$100 pc (e.g. Armstrong, Cordes & Rickett 1981). Such fluctuations could be expected to average out over longer path lengths.

As can be seen in Fig. 3, our electron distribution model depends to a large extent on pulsars at distances >1 kpc from the Sun. If the Sun happened to be located near a local minimum in the interstellar electron density, the effect on the low end of the derived pulsar luminosity function would be large in that the distances to most low-luminosity pulsars would be underestimated, and

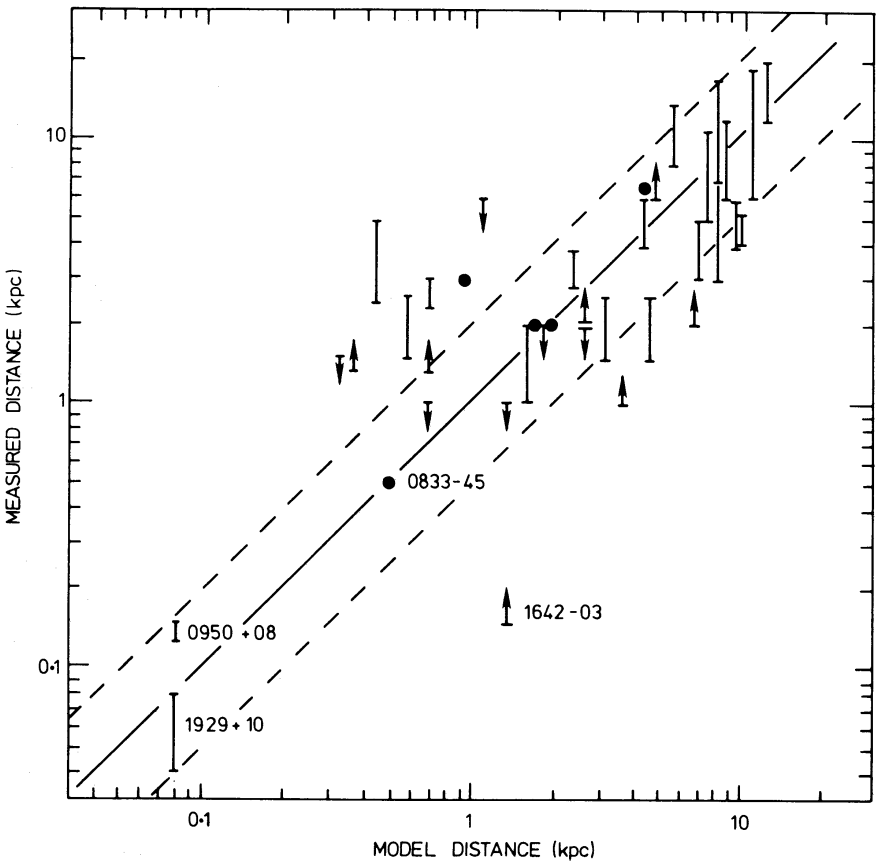

Figure 3. Measured distances of pulsars plotted against distances computed from dispersion measure and the adopted electron density model. Dashed lines bracket the line of equality by a factor of 2 in either direction.

hence their space density overestimated. Models of the soft X-ray background (e.g. Cox & Anderson 1982) suggest that the Sun may be located near a density minimum of the hot, X-ray emitting electrons. However, the pulsar parallax measurements by Salter, Lyne & Anderson (1979), Taylor *et al.* 1984, and Gwinn (1984) show that for the region within 1 kpc of the Sun, $n_e \approx 0.03\,\mathrm{cm}^{-3}$, essentially the same as the mean value found over larger distances. It appears, therefore, that most of the dispersing electrons are located in higher density (probably fully ionized) regions, and not in the hot or 'coronal' component of the interstellar medium. The distribution of the dispersing electrons is apparently reasonably uniform when averaged over scales larger than a few hundred parsecs.

Individual pulsar distances estimated by use of the model may occasionally be in error by as much as a factor of 2, because of peculiarities along a particular line-of-sight. A typical random error, however, is probably closer to a factor of 1.5, and the overall bias in the scale is probably not much more than the ~20 per cent uncertainty typical of other methods of reckoning galactic distances.

3 Spatial and luminosity distributions

In order to obtain a quantitative statistical description of the galactic population of pulsars, we have evaluated the selection effects relevant to the four most extensive pulsar surveys undertaken at Jodrell Bank, Arecibo, Molonglo, and Green Bank. These surveys detected a total of 316 pulsars, the parameters of which thus comprise our basic observational data. Each survey had different sky coverage and a different dependence of sensitivity on dispersion measure; it is such

details that must be evaluated quantitatively in order to extrapolate from the observed pulsar sample to the characteristics of the population as a whole.

The four surveys also had somewhat different dependences of sensitivity on period. These differences are not very important for our present purpose because the sensitivity of each survey was nearly uniform throughout the period range that characterizes the overwhelming majority of pulsars. Further details concerning period-sensitive selection effects are presented in Appendix A and discussed in Section 4.1

The basic observational data for each of the 316 sample pulsars include the galactic coordinates l and b, the dispersion measure DM, and the mean flux density at 400 MHz, S_{400}. As described in Section 2, we have (with a few exceptions) adopted the distances d given by Manchester & Taylor (1981). From l, b, and d we transform to the equivalent set of galactocentric cylindrical coordinates R, θ, and z. We assume that the Galaxy is axially symmetric, so the θ coordinate is not subsequently used. In keeping with past practice (e.g. Taylor & Manchester 1977) and because no better measure is generally available, we adopt the simple measure $L=S_{400}\,d^2$, with S_{400} in mJy and d in kpc, as an estimate of the radio luminosity of a pulsar.

Armed with the R, z, and L parameters of 316 observed pulsars, we can proceed to estimate the distribution functions of the parent population. We have followed the basic method used by Taylor & Manchester (1977), solving for spatial density functions $\varrho_R(R)$ and $\varrho_z(z)$ and the luminosity function $\Phi(L)$. We begin by estimating the volume of the Galaxy, $V(R, z, L)$, that the four surveys have effectively searched for pulsars of coordinates R, z and luminosity L. We use a numerical approach, and divide the parameter space into 20 zones of R, each 1 kpc wide; 30 zones of z, each 0.1 kpc thick; and 15 logarithmic zones of L, each half a decade wide. Details on the computation of the 9000 values of $V(R, z, L)$ are given in Appendix B. Our procedure assumes that the three distribution functions ϱ_R, ϱ_z, and Φ are independent. This assumption appears fully justified in the case of ϱ_R, but there are grounds for considering a correlation between z and L. As discussed below, pulsars are apparently born near the galactic plane and, on the average, move to higher z-distances during their lifetime. At the same time, their luminosity is believed to decay. Consequently, high-z pulsars will generally be of low luminosity. The effect of neglecting this dependence will be to underestimate the true width of the pulsar z distribution. To some extent, this effect will be compensated by the tendency of high-velocity pulsars to have strong magnetic fields (Anderson & Lyne 1983) and hence higher than average luminosities. Unfortunately, the number of observed pulsars is insufficient to quantify these effects.

The observed distributions $N_R(R)$, $N_z(z)$, and $N_L(L)$ of the 316 sample pulsars are plotted as histograms in the top portions of Figs 4–6. Corrected distribution functions for the parent population were obtained by using the equations

$$\varrho_R(R)=\frac{N_R(R)}{\sum_z\sum_L V(R,z,L)\varrho_z(z)\Phi(L)} \tag{3.1}$$

$$\varrho_z(z)=\frac{N_z(z)}{\sum_R\sum_L V(R,z,L)\varrho_R(R)\Phi(L)} \tag{3.2}$$

$$\Phi(L)=\frac{N_L(L)}{\sum_R\sum_z V(R,z,L)\varrho_R(R)\varrho_z(z)} \tag{3.3}$$

and iterating several times. In these equations the summations are taken over the 20, 30, and 15

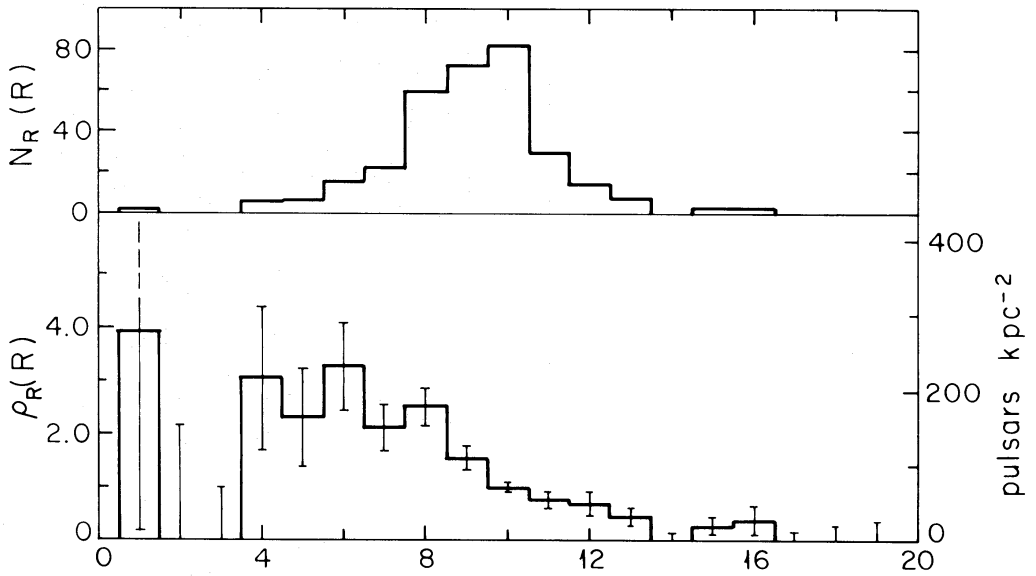

Figure 4. Distribution of sample pulsars with respect to galactocentric radius R, and the derived radial density function $\varrho_R(R)$ normalized to unity at $R=10$ kpc. The right-hand scale gives the corresponding surface density of pulsars integrated over z at the solar distance, $R=10$ kpc.

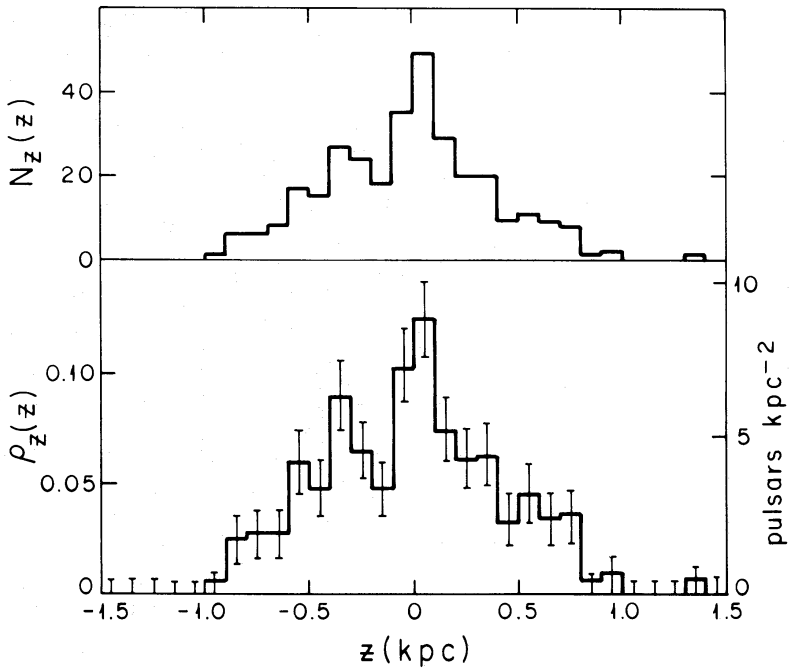

Figure 5. Distribution of sample pulsars with respect to distance z from the galactic plane, and the derived function $\varrho_z(z)$ normalized so that it sums to unity. The right-hand scale gives the corresponding density of pulsars in each z-interval at the solar distance, $R=10$ kpc. The Sun is assumed to lie at $z=0$.

bins, respectively, of R, z, and L. The iterative procedure converges rapidly for any reasonable starting values of the functions.

We choose to normalize the three distribution functions so that

$$\varrho_R(10\,\text{kpc})=\int_{-\infty}^{\infty}\varrho_z(z)\,dz=1. \tag{3.4}$$

With this convention, the dimensions of $\Phi(L)$ are pulsars per kpc^2 per luminosity interval, and the values of $\Phi(L)$ refer to the solar neighbourhood, i.e. $R=10$ kpc and $z=0$. Fig. 3 and the

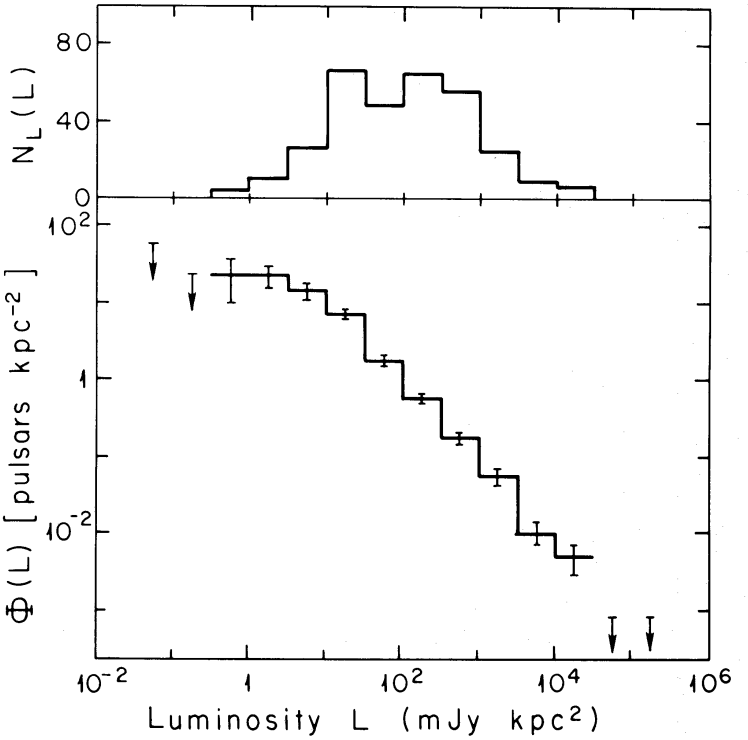

Figure 6. The distribution of sample pulsars with respect to radio luminosity L, and the derived luminosity function in the solar neighbourhood, $\Phi(L)$.

accompanying text in Section 2 showed that the typical error in the distances assigned to pulsars in our sample is a factor in the range ~0.7 to 1.5. Because the number of sample pulsars within a radial distance r increases roughly as the square of r, at least for $r \lesssim 1$ kpc, a random distribution of distance errors produces a biased estimate of the local density of pulsars (Morini 1981); a greater number of distant pulsars are assigned nearby distances than vice-versa, simply because there are more of them. It is easy to show that if the distance errors have an unbiased Gaussian distribution in their logarithm, with a standard deviation of 2 dB (corresponding to the factor of 1.5 mentioned above), the resulting bias in $\Phi(L)$ is a factor of about 1.5. To correct for this bias, we have reduced each estimated value of $\Phi(L)$ by this factor.

Final results for the three distribution functions are plotted in the lower portions of Figs 4–6, with error bars that give statistical estimates of the uncertainties involved. For the R and z distributions the left-hand scales give the actual values of $\varrho_R(R)$ and $\varrho_z(z)$, while the right-hand scales give these values multiplied by the total density of potentially observable pulsars in the solar neighbourhood,

$$\int_{L_{\min}}^{\infty} \Phi(L) \frac{dL}{L} = 70 \pm 15 \text{ kpc}^{-2}, \tag{3.5}$$

where $L_{\min}$ is taken as 0.3 mJy kpc^2.

The corresponding total number of observable pulsars in the Galaxy can be obtained from the integral

$$N_G = \int_{-\infty}^{\infty} \varrho_z(z)\, dz \int_0^{\infty} 2\pi R \varrho_R(R)\, dR \int_{L_{\min}}^{\infty} \Phi(L) \frac{dL}{L}. \tag{3.6}$$

With our normalization scheme the first integral reduces to unity; the second integral, which represents the (weighted) area of the galactic disc occupied by pulsars, has the value

$1000\pm100\,\mathrm{kpc}^2$. The product of the three integrals gives $N_G=(0.70\pm0.17)\times10^5$ potentially observable pulsars of luminosity $L>0.3\,\mathrm{mJy\,kpc}^2$ in the Galaxy, where the quoted error represents only the statistical uncertainty.

In order to test the effect of systematic errors in the distance scale, we repeated the calculations with the interstellar electron densities scaled both up and down by 20 per cent. For a factor f change in the distance scale, the local surface density of pulsars (equation 3.5) varies as f^{-2}. However, the effective size of the galactic pulsar disc varies approximately as f, so the net effect on the total inferred population is a factor f^{-1}. As stated in Section 2, we believe the systematic error in the distance scale to be $\lesssim$20 per cent, so this uncertainty also applies to the total pulsar population.

4 Evolution and birthrate

The size of the galactic population of pulsars inferred in Section 3 is determined by the pulsar birthrate and by the lifetimes of pulsars: that is, the rate at which the luminosities rise above, and the length of time they remain above, the lower luminosity limit of $L_{\min}\approx0.3\,\mathrm{mJy\,kpc}^2$. Also, the observed distribution of periods and period derivatives is closely linked with the evolution of luminosities because of selection effects. Measurements of period derivatives have now been obtained for most of the pulsars found in the major surveys (Gullahorn & Rankin 1978; Ashworth & Lyne 1981; Newton *et al.* 1981; Backus *et al.* 1982), and the results are summarized by Manchester & Taylor (1981). In this section we analyse a sample of 265 pulsars consisting of all

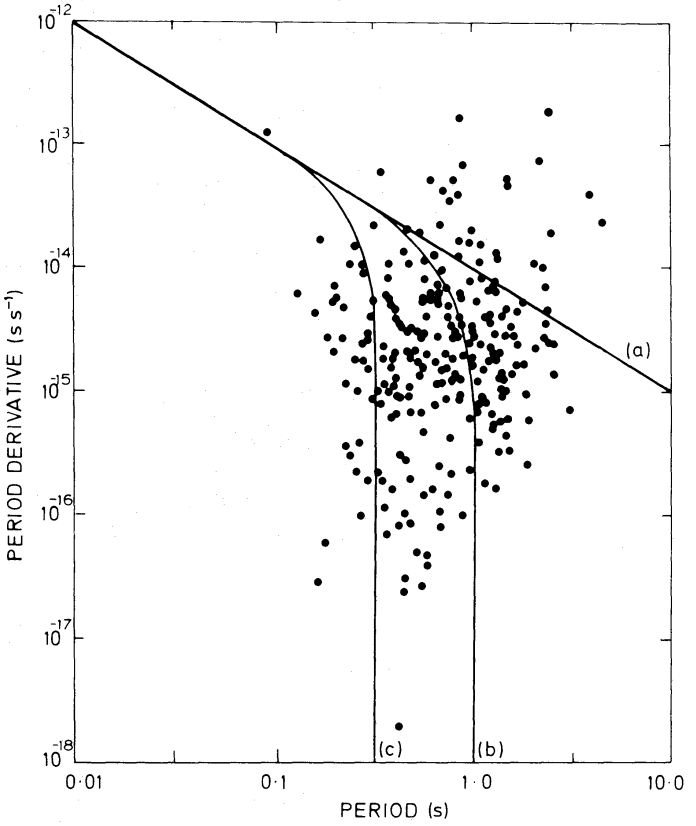

Figure 7. The observed P–$\dot{P}$ diagram for the flux-limited sample of 265 pulsars. Also shown are the evolutionary paths of a single pulsar for (a) constant magnetic field, and for field decay times of (b) 10 Myr and (c) 1 Myr. For stronger or weaker initial magnetic fields, this family of curves would be higher or lower by half a decade in both P and $\dot{P}$ for each decade in magnetic field.

pulsars used in the previous section having known period derivatives, except those detected only in the Arecibo survey. These 265 pulsars constitute an approximately flux-limited sample.

Fig. 7 is a plot of period P against period derivative $\dot{P}$ for our sample. Most of these pulsars are thought to have been born with small periods and large period-derivatives, placing them near the top left-hand corner of the diagram. After birth, if a pulsar's magnetic field remains constant, energy and angular momentum loss due to magnetic dipole radiation (Pacini 1967, 1968; Ostriker & Gunn 1969) will result in an evolution downward along lines parallel to the one labelled (a) in the figure, at a rate that varies inversely with the period. On the other hand, if the magnetic field decays exponentially, the expected evolutionary track will steepen and eventually become vertical, as in lines (b) and (c). Each pulsar would thus reach a 'terminal period' at which its magnetic field has decayed to a small value (Lyne *et al.* 1975).

A commonly used indicator of the age of a pulsar has been the characteristic or 'spin-down' age, $\tau=P/(2\dot{P})$, which is equal to the chronological age if the effective magnetic dipole moment has remained constant and if the pulsar's period at birth was much less than the present period. Studies of the distribution of pulsars in the P–$\dot{P}$ diagram (Lyne *et al.* 1975), however, have suggested that the magnetic moment of a pulsar decays during its lifetime and that the larger values of characteristic age are substantial overestimates of the true ages. This conclusion is strongly reinforced by kinematic estimates of pulsar ages derived from proper motion measurements (Manchester *et al.* 1974; Lyne *et al.* 1982).

The distribution of points in Fig. 7 immediately implies some kind of luminosity evolution. In particular, the maximum in the period distribution at ~0.6 s shows that ageing eventually causes a pulsar's radio luminosity to fall below the level of detectability from Earth. Observations of pulse nulling by Ritchings (1976) suggested that the deaths of pulsars may be rather abrupt. For this reason, most recent models of pulsar evolution have involved the assumption of constant luminosity until a cut-off line of the form $\dot{P}\propto P^{\alpha}$ was reached in the P–$\dot{P}$ diagram (see, for example, Fujimura & Kennel 1980; Phinney & Blandford 1981). On the other hand, an actual (or even an apparent) decay of the magnetic field probably results in a more gradual decay of the effective pulsed luminosity, as was first suggested by Gunn & Ostriker (1970). In this section we therefore investigate the implications of magnetic field and luminosity evolution using a much larger sample of pulsars than has been available in the past.

4.1 PERIOD AND LUMINOSITY EVOLUTION

We consider first a model in which the magnetic field, B, decays and the luminosity is proportional to B^2. Such an evolution was first discussed by Gunn & Ostriker (1970), and we follow their approach in the treatment given below.

Let us assume that a pulsar is born with an initial surface magnetic field $B_{\rm i}$ which decays exponentially with a time-scale t_B. After a time t the magnetic field is thus

$$B=B_{\rm i}\exp(-t/t_B). \tag{4.1}$$

For a dipolar magnetic field structure we have

$$P\dot{P}=AB^2=AB_{\rm i}^2\exp(-2t/t_B) \tag{4.2}$$

where the constant $A=9.8\times10^{-40}\,{\rm s\,G^{-2}}$ for a stellar moment of inertia of $10^{45}\,{\rm g\,cm^2}$ and radius of $10^6\,{\rm cm}$. This equation can be integrated to determine the variation of period with time,

$$P^2=At_BB_{\rm i}^2[1-\exp(-2t/t_B)]=P_{\rm t}^2[1-\exp(-2t/t_B)] \tag{4.3}$$

where $P_{\rm t}$ is the terminal period, that is, the rotation period after the magnetic field has decayed to

zero. P_t is related to the initial magnetic field by

$$P_t=(At_B)^{1/2}B_i. \tag{4.4}$$

This quantity may be determined from the observed period and period derivative by the relation

$$P_t=P+\dot{P}t_B. \tag{4.5}$$

In the presence of field decay the characteristic age varies non-linearly with time; from equations (4.2) and (4.3) we obtain

$$\tau=\frac{P}{2\dot{P}}=\frac{1}{2}t_B[\exp(2t/t_B)-1]. \tag{4.6}$$

The true age t can be determined by re-arranging equation (4.6) to yield

$$t=\frac{1}{2}t_B\ln\left(\frac{2\tau}{t_B}+1\right). \tag{4.7}$$

These equations describe the evolution of the magnetic field and period of an individual pulsar. Gunn & Ostriker suggested taking the initial magnetic fields of the population as a whole to have a Gaussian distribution in the logarithm of B_i, with a standard deviation σ about a mean in $\ln \bar{B}_i$. The terminal periods will then be distributed in a similar manner (see equation 4.4), with the same σ and a mean of $\ln \bar{P}_t=\ln \bar{B}_i+\frac{1}{2}\ln(At_B)$.

Finally, Gunn & Ostriker make the plausible assumption that pulsar radio luminosities depend upon the square of the surface magnetic field, that is,

$$L=4\pi\beta B^2=4\pi\beta B_i^2\exp(-2t/t_B), \tag{4.8}$$

where β is a constant. They then consider what form the observed distributions of various quantities should take for a flux-limited sample in a planar galaxy. For example, the expected distributions in τ, P_t, and P are

$$N(\tau)\,d\tau=\frac{K_1\tau}{(1+2\tau/t_B)^2}\frac{d\tau}{\tau} \tag{4.9}$$

$$N(P_t)\,dP_t=K_2\exp\left\{\frac{-[\ln(P_t/\bar{P}_t)-2\sigma^2]^2}{2\sigma^2}\right\}\frac{dP_t}{P_t} \tag{4.10}$$

$$N(P)\,dP=K_3P^2\,\mathrm{erfc}\left[\frac{\ln(P/\bar{P}_t)}{\sqrt{2}\sigma}\right]\frac{dP}{P} \tag{4.11}$$

where K_1, K_2, and K_3 are normalization constants which depend on the number of pulsars in the flux-limited sample.

Fig. 8 shows the observed distribution of characteristic ages τ for the 265 pulsars in our actual, approximately flux-limited sample. The smooth solid curve shows the expected distribution for $t_B=9.1$ Myr, a value obtained from a least-squares fit of equation (4.9) to the data. Obviously this model, which (apart from a scaling factor) has only a single free parameter, is an excellent fit to the data. The terminal periods P_t were then calculated for each pulsar using equation (4.5) and $t_B=9.1$ Myr; their distribution is shown in Fig. 9. A least-squares fit of equation (4.10) to these data provides another excellent fit, and gives $\bar{P}_t=0.40\pm0.04$ s and $\sigma=0.69\pm0.03$. These parameters then determine the distribution of initial fields B_i through equation (4.4), and we find that $\bar{B}_i=0.75\times10^{12}$ G. Note that these mean values for P_t and B_i are for the population as a whole and not for the observed sample.

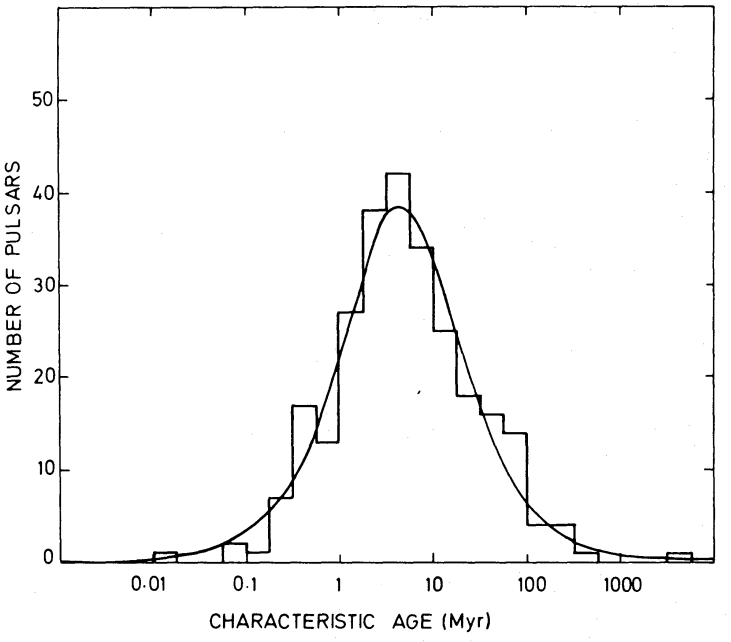

Figure 8. The observed distribution of characteristic ages τ and the fit to these data on the assumption that the luminosity is proportional to B^2. The derived value for the magnetic field decay time is t_B=9.1 Myr.

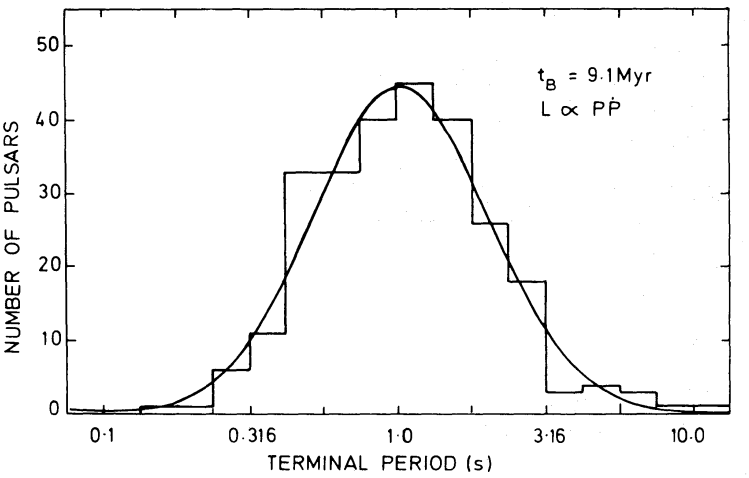

Figure 9. The observed distribution of terminal periods P_t for t_B=9.1 Myr. Since $B_i \propto P_t$, the histogram reflects the distribution of initial magnetic fields of the observed pulsars. The smooth curve is a least-squares fit of a distribution for the parent population which is Gaussian with standard deviation of 0.69 in the logarithm and has a mean initial magnetic field of 0.75×10^{12} G.

The Gunn–Ostriker model also predicts the distribution of pulsars in the P–$\dot{P}$ diagram with reasonable accuracy without invoking any arbitrary luminosity cut-off. Fig. 10(a) and (b) show the observed distribution and a Monte Carlo simulation of the distribution expected from the model outlined above. The simulation displays all the most prominent features of the observed distribution, including a sloping cut-off line to the right of the figure and an absence of small P, small $\dot{P}$ pulsars towards the bottom left.

In a more quantitative comparison, Fig. 11 illustrates the observed and expected period distributions, again using the model described above (equation 4.11). The agreement is satisfactory, especially when account is taken of instrumental bias against the detection of short-period pulsars (see Appendix A). The small deficit of pulsars with periods less than about 0.2 s can be accounted for by the effects of dispersion and interstellar scattering upon the survey

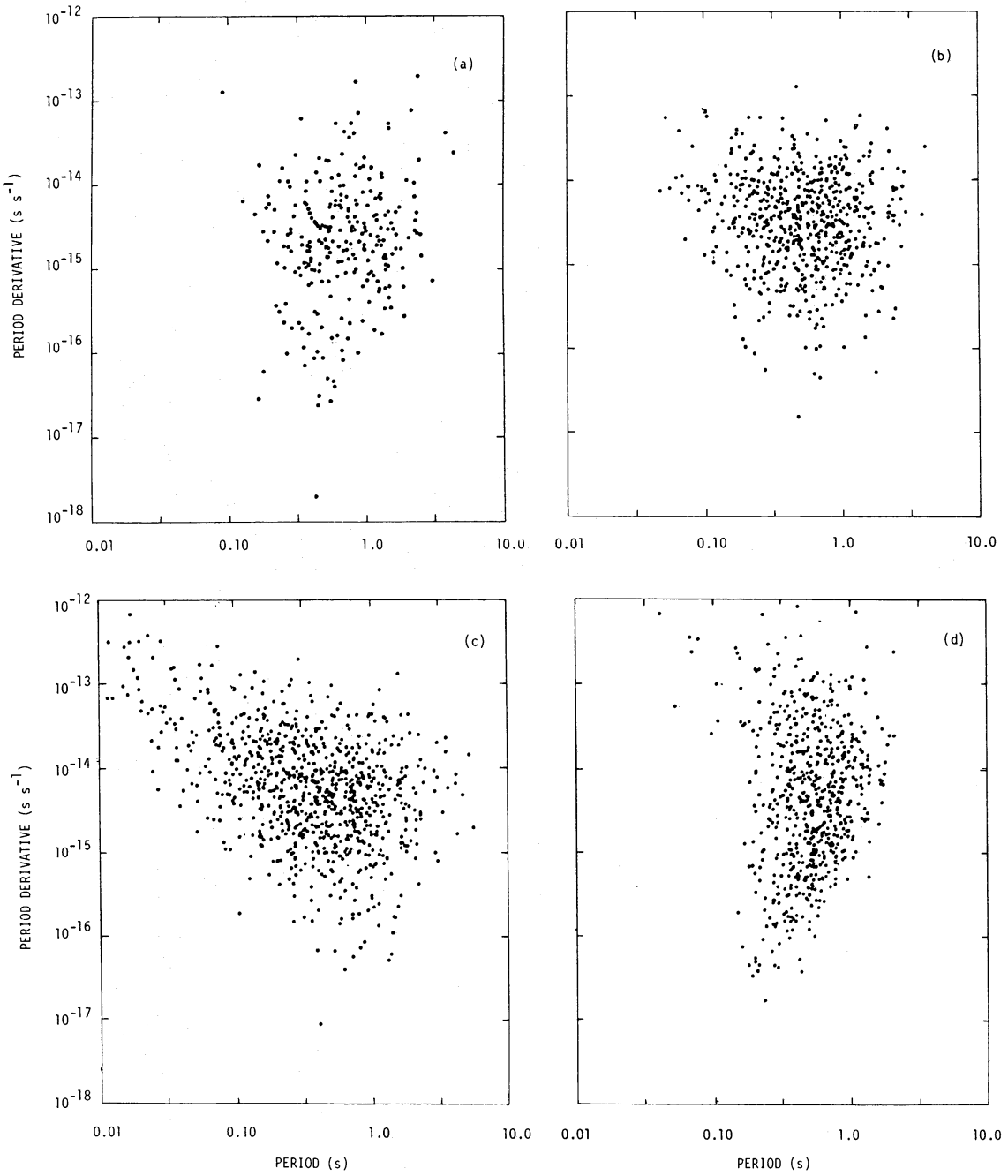

Figure 10. The observed distribution of pulsars in the P–$\dot{P}$ diagram (a), compared with Monte Carlo simulations for three different models: (b) t_B=9.1 Myr, $L \propto B^2$; (c) t_B=9.1 Myr, $L \propto B^2/P$; and (d) t_B=0.6 Myr, L constant until the cut-off line $\dot{P}P^{-2.75}=5\times10^{-6}$, with a Gaussian dither of standard deviation 0.69 in the logarithm of the cut-off parameter. The simulations (b–d) contain approximately twice as many points as the observed distribution, (a).

sensitivities. We estimate from Fig. 11 that a total of about 20 pulsars with periods <0.2 s have been rendered invisible this way. These 'missing' pulsars are likely to be young, luminous objects at large distances, and therefore particularly prone to the effects of pulse broadening in the interstellar medium.

Fig. 12 compares the observed and expected dependences of the luminosity L on characteristic age τ for the model discussed above, $L \propto P\dot{P}$. This figure provides the most direct available evidence for luminosity decay and again the agreement between model and data is satisfactory.

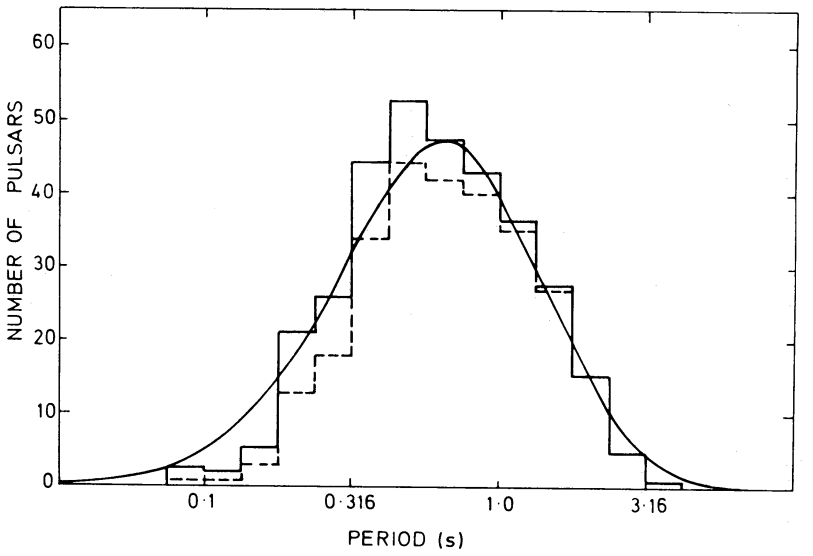

Figure 11. The observed and expected period distributions. The observed distribution (broken line histogram) has been corrected for the known dependence of sensitivity on period to give the solid line histogram. The curve shows the distribution expected with t_B=9.1 Myr, $\bar{B}_i$=0.75×10^{12} G and σ=0.69, that is, using the parameters derived from fits to the τ and P_t histograms.

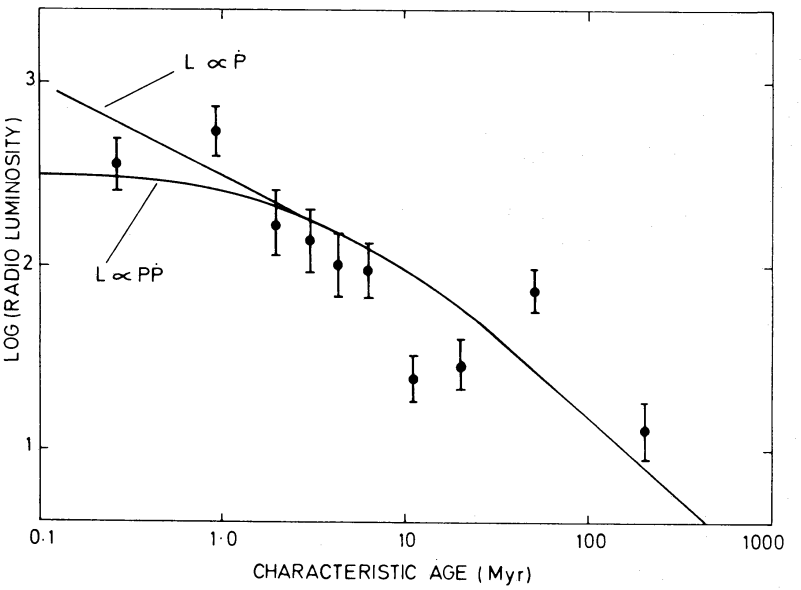

Figure 12. The evidence for luminosity decay. The mean luminosities of ordered groups of the observed pulsars are shown as a function of characteristic age τ. The two curves show the expected variation for models in which the magnetic field B decays exponentially with t_B=9.1 Myr and the luminosity is proportional to $P\dot{P}$ or B^2, and $\dot{P}$ or B^2/P.

As we have shown, the Gunn–Ostriker model, in spite of its simplicity, is remarkably good in describing the observed distributions. Of course, the model depends upon the assumption that pulsar luminosities are proportional to B^2 and therefore to $P\dot{P}$. A dependence of L on B can be seen directly in our sample, there being a marginally significant correlation coefficient of 0.17±0.06 between the logarithms of the two quantities. It is difficult to test the relationship quantitatively, however, because of the large scatter in L for a given value of B. The scatter is not unexpected, and is at least partly the result of a combination of beaming effects and errors in pulsar distances. Observational selection against intrinsically faint pulsars also biases the distribution.

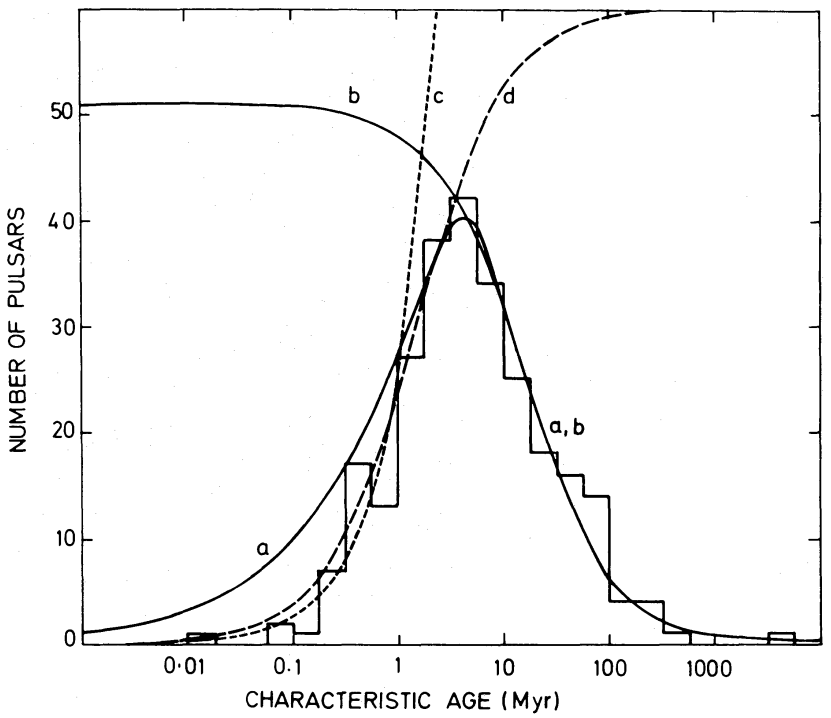

Figure 13. The observed distribution of characteristic ages τ compared with that expected for (a) $L \propto B^2/P$, t_B=12.7 Myr; (b) $L \propto B^2/P^2$, t_B=31.3 Myr; (c) L=constant, $t_B=\infty$; and (d) L=constant, t_B=3 Myr. For (a) and (b), the parameters (t_B and scaling factor) were determined by fitting to the high-τ side of the histogram and, for (c) and (d), to the low-τ side.

We have investigated the possibility that the luminosity depends upon some other function of P and $\dot{P}$. As shown in Figs 10 and 13, we find that the quality of the fits is quite sensitive to the assumed functional form. For example, a simple argument suggests that the luminosity might be proportional to the product of the magnitude of the electric field (determining the particle energy) and the magnetic field, leading to $L \propto B^2/P \propto \dot{P}$. The fitting procedures have been repeated for this model, and the results are presented for comparison with the observed data in Figs 10(c), 12, and 13(a). For comparison, fits based on luminosity proportional to $B^2/P^2 \propto \dot{P}/P \propto \tau^{-1}$ (Fig. 13b), constant luminosity and no magnetic field decay (13c), and constant luminosity and field decay with a time-scale of 3.1 Myr (13d), are shown. In case (c) the number of pulsars per logarithmic bin of τ is proportional to τ. In each of these cases the fits are distinctly poorer than the model fit shown in Fig. 8. For cases (a) and (b), there is an observed deficit of young, short-period pulsars. Certainly there are some selection effects (dispersion or scattering broadening, as discussed earlier) which might cause some under-counting of short-period pulsars, although it is difficult to believe that the surveys used in this analysis have detected only one tenth of the pulsars younger than 200 000 yr which are above the limiting flux density. The $L \propto B^2/P$ model might be acceptable if one were to invoke the injection of pulsars into the population at a finite age, as suggested by Phinney & Blandford (1981) and Vivekanand & Narayan (1981), but the $L \propto B^2$ model is perhaps preferable since it is consistent with the data without additional *ad hoc* assumptions.

Another type of model which has been considered is that in which the magnetic field decays but the luminosity remains constant until an abrupt cut-off (presumably due to pulse nulling) occurs near the observed right-hand edge of the distribution in the P–$\dot{P}$ diagram (Fujimura & Kennel 1980). A similar model, also invoking an abrupt luminosity cut-off, was described by Phinney & Blandford (1981). These models involve magnetic decay time constants of 10^6 yr or less. An example of the P–$\dot{P}$ distribution resulting from such models, where we have used parameters

derived by Fujimura & Kennel (1980), is shown in Fig. 10(d). The parameters of this model were effectively determined by a fit to the period distribution. However, Fig. 10(d) shows that the predicted P–$\dot{P}$ distribution has a different character from that observed. In particular, there is a strong relative excess of pulsars with large characteristic ages, even when a normally distributed 'dither' is introduced into the cut-off parameter.

These 'luminosity cut-off' models were motivated primarily by the observation by Ritchings (1976) that many pulsars close to the right-hand edge of the distribution in the P–$\dot{P}$ diagram display nulling – the complete absence of radiation for one or more consecutive pulsar periods. Moreover, the closer to the cut-off line, the greater is the fraction of time spent by a pulsar in its nulled state, suggesting that pulsars die when this fraction reaches unity. It is difficult to conceive of a emission mechanism in which the luminosity remains constant as the magnetic field and period of the pulsar evolve. It may be that all pulsars do finally die through nulling, but it seems that the main reason for the low density of pulsars on the right-hand side of the P–$\dot{P}$ diagram is the steady decay of luminosity with time that we see in Fig. 12. This is supported by the fact that the pulsars which are observed to null are concentrated close to the right-hand edge of the P–$\dot{P}$ diagram (Ritchings 1976) whereas the density begins to fall well to the left of this. We believe that nulling itself is responsible for only a very small decrease in the luminosities of the observed pulsars, and that most pulsars disappear from the P–$\dot{P}$ diagram when their luminosity falls gradually below that at which they are detectable from the Earth.

4.2 THE z-DISTRIBUTION

The distribution of pulsars in distance from the galactic plane, z, provides a further check of luminosity evolution models. Proper motion measurements have demonstrated that pulsars have substantial space velocities; Lyne *et al.* (1982) have shown that they are generally directed away from the plane and have a quasi-Maxwellian amplitude distribution with a z-component dispersion of 107 km s^{-1}. The observations are consistent with most pulsar births occurring close to the galactic plane, within the distribution of extreme Population I objects. Pulsars therefore move some distance away from the galactic plane before their luminosities fall below $L_{\min}$ and they effectively die.

The combination of these effects must determine the form of the observed z-distribution, as presented in Fig. 5. Gunn & Ostriker have shown how the model distribution of pulsars may be expected to vary as a function of z distance and age t, for a Maxwellian distribution of velocities. Multiplying this distribution by the number of pulsars that still have luminosities exceeding $L_{\min}$ at a given age t, and integrating over all ages, provides an estimate of the true z-distribution. The model distribution derived in this way is compared with the corrected $|z|$ distribution (*c.f.* Fig. 5) in Fig. 14. Luminosities are assumed to decay with the square of the surface magnetic field, and hence on a time-scale of $t_B/2=4.55$ Myr. On the whole the agreement is good, and the observations certainly do not conflict with the model we have described.

4.3 THE PULSAR BIRTHRATE

In Section 3 we derived the volume density of pulsars in the solar neighbourhood as a function of luminosity. Since we now have a model for the decay of pulsar luminosity with time, it is straightforward to estimate the rate at which pulsars must be born in order to keep the luminosity function constant in time.

On the assumption that pulsar luminosities decay with an exponential time-scale of 4.55 Myr, pulsars will evolve from right to left in Fig. 6. All the pulsars in one semi-decade luminosity bin will move into the next bin in a time of $4.55\ln(\sqrt{10})=5.2$ Myr. Since pulsar lifetimes are short

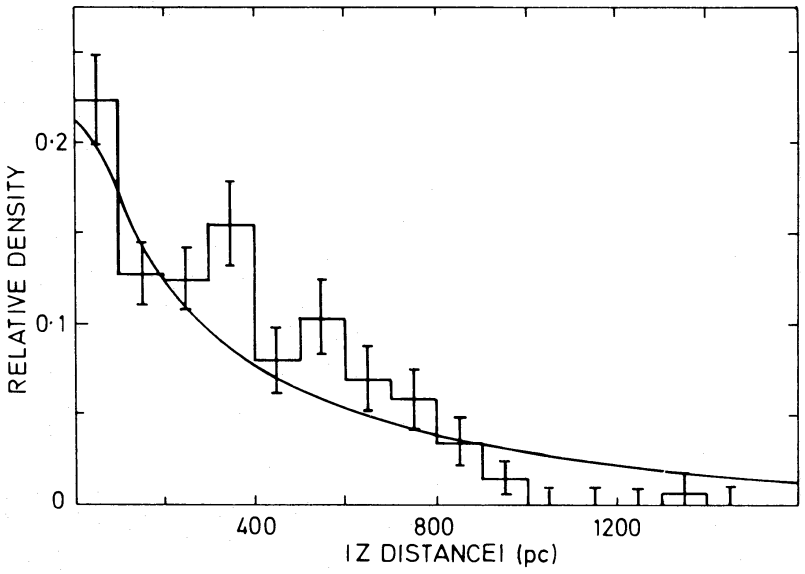

Figure 14. The $|z|$ distribution of pulsars, corrected for selection effects, and the predicted distribution. The prediction is based on $L \propto B^2$, t_B=9.1 Myr, and a Maxwellian distribution of pulsar velocities having a standard deviation of 107 km s^{-1}.

compared with the age of the Galaxy, it is reasonable to assume stationarity in the pulsar population. Therefore, in order to maintain the same form of the luminosity function, pulsar births during an interval of 5.2 Myr must make up the difference between the number of pulsars in a given luminosity bin and those in the next higher bin. The flattening of the luminosity function around $L \sim 1$ mJy kpc^2 suggests that few pulsars are born with luminosities less than this value. The maximum rate of flow of pulsars is thus determined by the most populous bin, which contains 22 ± 7 pulsar kpc^{-2}. All of these pulsars must move into the next lower bin within 5.2 Myr, and must be replaced in a steady-state situation. We are thus led to a minimum birthrate of 4.3 ± 1.3 kpc^{-2} Myr^{-1} in the solar neighbourhood, the uncertainty being a purely statistical estimate.

We emphasize that this birthrate is a lower limit in the sense that it assumes that no pulsars die other than through the mechanism of gradual luminosity decay. In addition, our birthrate figure does not take account of any pulsars born with effective luminosities (directed toward the Earth) less than 1 mJy kpc^2. Such intrinsically weak pulsars may exist, but recent observations by Dewey (1984) suggest that they are not very numerous.

The galactic birthrate can now be obtained by integrating through the Galaxy in the same way as we did for the calculation of the total population. The integral gives 4300 pulsar Myr^{-1}, or one pulsar birth every 230 yr. It is generally believed that pulsar beams sweep over only a fraction of the celestial sphere, although the magnitude of the fraction is a matter of controversy. A value of 0.2, based on the observed longitude width of pulse profiles and the assumption of beam circularity, has often been assumed (e.g. Davies *et al.* 1977). Narayan & Vivekanand (1983), however, argue that pulsar beams are elongated in the latitude direction and, furthermore, that the degree of elongation is a function of period. Integrating their relationship for beam elongation over the (corrected) period distribution (Fig. 11) gives a mean value of approximately 2.5. This would increase the effective beaming fraction to about 0.5. Taking account of the various uncertainties, we arrive at a final birthrate estimate of one pulsar every 30 to 120 yr somewhere in the Galaxy.

The calculated birthrate for each of our semi-decade luminosity classes is shown in Fig. 15, along with a fit of the Gaussian distribution of initial luminosities expected on the basis of a

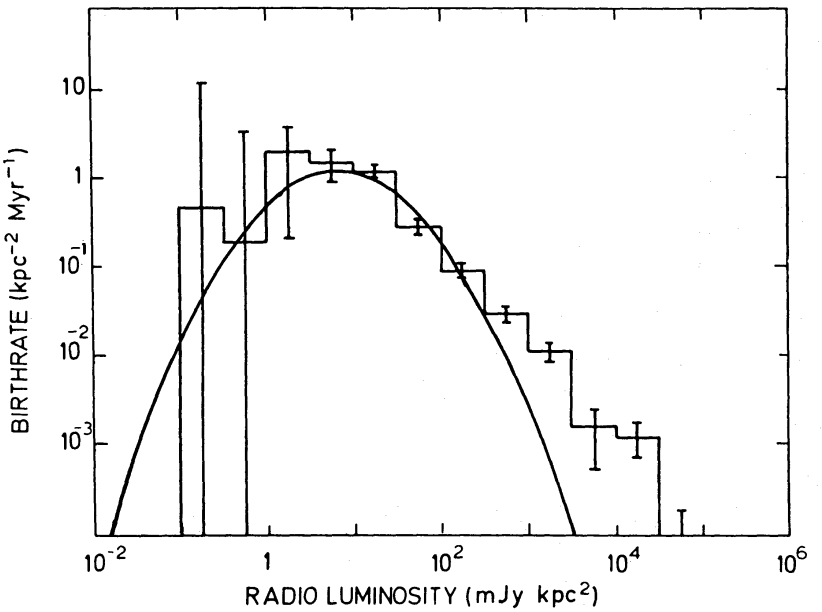

Figure 15. The birthrate of pulsars in the neighbourhood of the Sun as a function of radio luminosity L, together with the distribution of initial luminosities expected on the basis $L \propto B^2$ and a Gaussian distribution of initial magnetic fields.

Gaussian distribution of initial magnetic fields and equation (4.8). The predicted distribution, which has a standard deviation of $2\sigma = 1.38$ in the logarithm, is a satisfactory fit to the data over most of the range and gives a mean initial luminosity of about 8 mJy kpc^2, more than an order of magnitude smaller than the mean luminosity of pulsars in a typical flux-limited sample (see Fig. 6, top). Differences between the zero-age luminosity distribution and the initial magnetic field distribution would result from the differing orientations of pulsar beams with respect to the Earth. Only if all pulsars were beamed towards Earth and had the same beamwidth in latitude and longitude would the luminosities computed in Section 3 be in any sense a direct measure of the radio luminosity. In practice, the true luminosities will all be greater than or equal to those observed.

5 Discussion and conclusions

In Section 2 we described a method for estimating pulsar distances; Section 3 presents a computation of the radial (R) and vertical (z) distributions of pulsars in the Galaxy, and the luminosity function; and Section 4 gives a description of pulsar evolution in terms of a simple but plausible physical model. As a product of these results, we have also estimated the rate at which pulsars must be born in order to maintain the inferred numbers throughout the Galaxy. How believable are these results, and how well do they fit in with the best current understanding of stellar evolution and galactic dynamics?

Let us first address the question of pulsar distances. We have based our distance scale on the pulsar dispersion measures and an interstellar electron density model. The model consists of (1) a component, with a small scale-height, representing the average of H II regions, (2) a component of uniform electron density, and (3) a component representing the dispersion contribution of the Gum Nebula. The first two components have a weak dependence on galactocentric radius R. More elaborate models have been devised for the large-scale distribution of free electrons in the interstellar medium; for example, Guseinov, Kasumov & Yusifov (1982a) present a scheme based on the distribution of H II regions, H_2O masers, OB stars, and other extreme Population I

material. In a somewhat *ad hoc* manner, and partly to minimize the number of anomalous pulsar distances, they assign different values of $\langle n_e \rangle$ for 36 different zones of galactic longitude and distance from the Sun. We find the evidence for such a complicated model less than compelling, and much prefer a simple model such as ours with a small number of adjustable parameters.

In a more global approach, Harding & Harding (1982) argue for an increased density and decreased scale height of electrons at galactocentric radii inside ~7 kpc, and for an asymmetry in the distribution relative to the galactic plane. There are, of course, good reasons to expect conditions to be substantially different in the inner portions of the Galaxy. However, our computation of the space density of pulsars depends largely on objects within 2 or 3 kpc of the Sun. Adopting a different electron density model for the inner Galaxy would change the details of the radial distribution inside its peak (see Fig. 4), but would make little difference to the integrated galactic population.

As a final comment on pulsar distances, we note that our model, first described by Manchester & Taylor (1981), is nearly identical to the one obtained by Vivekanand & Narayan (1982) through a number of independent approaches. We believe it to be a reliable description of the large-scale features of the ionized interstellar medium within ~5 kpc of the Sun.

The distribution of pulsars as a function of galactocentric radius (Fig. 4) shows a peak in the zone 4–6 kpc and a roughly exponential fall-off in density through the solar radius and beyond. It is probable that the deduced densities for $R \lesssim 5$ kpc are somewhat less than the true values because of the effects of increased interstellar dispersion and scattering in the inner part of the Galaxy. Compared to other uncertainties, however, this introduces a negligible error into the derived total galactic population and birthrate since the fraction of the Galaxy within this radius is small. Fig. 4 implies that 70 per cent of all pulsars (with luminosity >0.3 mJy kpc^2) lie within the solar circle. This observed R distribution is similar to that for supernovae (Tammann 1982), supernova remnants (Clark & Caswell 1976), and molecular clouds (Robinson *et al.* 1984), reinforcing the association of pulsars with supernovae and Population I progenitors.

Unlike the R and L distributions (Figs 4 and 6), the galactic z distribution (Fig. 5) is only slightly affected by observational selection, so the observed and corrected histograms are very similar. The distribution can reasonably be approximated by an exponential function with scale height of about 400 pc. This is much more than the scale height of the massive stars thought to be the progenitors of pulsars, 70–90 pc (e.g. Miller & Scalo 1979), and hence is consistent with the observation that pulsars move substantial distances from their birthplaces during their lifetimes (Lyne *et al.* 1982). Fig. 14 shows that the z-distribution expected on this basis is close to that observed. Helfand & Tademaru (1977) suggested that pulsars were divided into two classes, one with low velocities and small scale height and the other with high velocities and large scale height. From Fig. 5, we can say that the excess number of pulsars in the lowest $|z|$ bins is $\lesssim 25$. Consequently, the low-velocity class, if it exists, contains less than 10 per cent of the observed population.

Consistent with earlier work (e.g. Taylor & Manchester 1977; Davies *et al.* 1977), the pulsar luminosity function (Fig. 6) is close to a power law with slope of -1 over most of its range. Thus, the galactic population is overwhelmingly dominated by intrinsically faint pulsars. For luminosities less than about 10 mJy kpc^2, however, the present work shows a significant decrease of slope. This result is important because it puts an upper bound on the number of pulsars in the Galaxy and hence on the birthrate. We note that the turnover at the low end of the luminosity function has been confirmed by the recent observations by Dewey (1984). Section 4 shows that the observed distribution and evolution of pulsars is still remarkably well described by the Gunn & Ostriker (1970) model, even though the observed pulsar sample has increased in size by an order of magnitude. This model is based on the proposition that the pulsar magnetic field B decays exponentially and that the radio luminosity also decays as B^2 or $P\dot{P}$. It predicts the

distribution of periods and period derivatives very well, while requiring a minimum of *ad hoc* assumptions. In particular, the general form of the observed P–$\dot{P}$ diagram is reproduced, the right-hand sloping 'cut-off' line being a natural feature of the model without the arbitrary 'death-line' required by others. In the absence of a self-consistent model of pulsar electrodynamics and the radio emission mechanism, the Gunn–Ostriker model at least provides a clear basis for interpretation of the phenomena involved. Fig. 12 provides some positive evidence for the hypothesis that radio luminosities decay exponentially with time. Despite this, other functional dependences of luminosity on P and $\dot{P}$ are also possible. If the power-law index of period dependence is less than one, then the apparent deficit of short-period pulsars becomes severe. For example, direct fits of a functional dependence of observed luminosities on P and $\dot{P}$ of the form $L \propto P^{\alpha}\dot{P}^{\beta}$ have been made by Lyne *et al.* (1975) and Vivekanand & Narayan (1981). Giving α between -2 and -1 and β between 0.4 and 0.9. Such a luminosity dependence would imply a large deficit of short-period pulsars which is unlikely to be accounted for by observational selection, and birth with long period or late turn-on of the pulsed emission (Phinney & Blandford 1981; Vivekanand & Narayan 1981) would have to be invoked. The determination of the coefficients α and β is very uncertain because of selection effects and the large scatter in L for a given P and $\dot{P}$, and it is not clear that they represent the trajectory of pulsar luminosity evolution. The variation of beam elongation with period proposed by Narayan & Vivekanand (1983) would produce an additional apparent inverse period dependence of luminosity and hence make the argument for late turn-on stronger.

Injection of pulsars into the galactic population at periods <0.5 s is not required in the self-consistent $L \propto B^2$ model described in Section 4. Vivekanand & Narayan (1981) argue on model-free grounds that injection is necessary, but this result is dependent on completeness of the major pulsar surveys at short period and is also subject to considerable statistical uncertainty. Vivekanand *et al.* (1982) suggest that selection effects do not significantly affect the conclusion that injection is required, but they do not include the effects of interstellar scattering. Manchester, D'Amico & Tuohy (1985) show that interstellar scattering is important and that many short-period pulsars are likely to have been missed in the large-scale surveys. The idea of injection has certain attractions: for example, it could account for the small number of observed pulsar–supernova remnant associations. Nevertheless, we do not believe that it is required by the observational data.

On the birthrate question, our analysis requires a minimum rate of one pulsar birth in the Galaxy every 230 yr. If the beaming factor is about five, then the required rate is greater than one birth every 50 yr. If pulsar beams are elongated and the degree of elongation is a function of period, then the required minimum rate drops to about one every 100 yr. Taking these effects into account, together with our estimates of the uncertainty in the distance scale, we arrive at a range of 30–120 yr for the mean interval between pulsar births in the Galaxy. This corresponds to a local birthrate in the range $(0.8\text{–}3)\times10^{-11}\,\mathrm{pc^{-2}\,yr^{-1}}$.

The derived mean interval between pulsar births is somewhat greater than a number of previous estimates (summarized by Lyne 1981) for three main reasons. First, the estimated distances to the nearest pulsars have been increased somewhat, mainly because we believe that previous values overestimated the effects of discrete H II regions on the dispersion measures. The result is a smaller estimated local density of pulsars, especially for the low-luminosity pulsars that are the most numerous ones in the Galaxy. Secondly, we have accounted for a significant bias in the estimate of local pulsar density caused by unbiased errors in the assigned distances to the known pulsars. Finally, we have shown that the large majority of galactic pulsars are old low-luminosity objects – considerably older than the ages typical of the observed sample, which is biased toward bright, young objects. It is wrong to deduce the lifetimes of the galactic population directly from the ages of pulsars in the highly biased observed sample.

From radio observations of supernova remnants, Clark & Caswell (1976) obtained a mean time between supernovae (of the type leaving shell-type remnants) of ~150 yr. Consideration of the more rapid evolution of remnants at high z distances led Caswell & Lerche (1979) to reduce this interval to ~80 yr. Further analyses considering the effects of a hot coronal component of the interstellar medium (Higdon & Lingenfelter 1980; Kafatos *et al.* 1980) led to estimates in the range 10–30 yr. More recently, Mills (1983) has derived a mean interval of about 30 yr from comparison with Magellanic Cloud supernova remnants. These values are consistent with the estimates based on observations of external galaxies (Tammann 1982) of one event every 20–40 yr and with estimates based on historical supernovae (Clark & Stephenson 1977; Srinivasan & Dwarakanath 1982) of 20–30 yr. They are also consistent with the pulsar birthrate derived in this paper.

From the stellar birthrate data of Miller & Scalo (1979), with the age of the Galaxy (T_0) taken to be 12×10^9 yr, our lower limit on the local pulsar birthrate, 0.8×10^{-11} pc^{-2} yr^{-1}, corresponds to the birthrate (or deathrate) of all stars with mass $M>16\,M_\odot$ or alternatively, to stars with masses in the range 8–10 $M_\odot$. The corresponding values for the pulsar upper limit, 3×10^{-11} pc^{-2} yr^{-1}, are $M>9\,M_\odot$ and $8<M<25\,M_\odot$. Stellar evolution calculations (e.g. Nomoto 1984; Hillebrandt, Nomoto & Wolff 1984) suggest that stars with masses in the range 8–10 $M_\odot$ will form neutron stars. There is some observational evidence (Reimers & Koester 1982; Wood, Bessell & Fox 1983) that stars with masses greater than 5 or 6 $M_\odot$ end their lives as supernovae. Some of these may leave neutron stars. At the higher mass end, estimates of heavy element production rates probably require stars as massive as 25 $M_\odot$ to form supernovae (e.g. Hillebrandt 1982). These supernovae are of Type II and would probably leave neutron star remnants. The deduced pulsar birthrates are therefore comfortably accommodated by theoretical models of stellar evolution and neutron star formation. The uncertainties in the various rates allow, but do not require, that some pulsars are born in 'quiet collapses' (e.g. Nomoto 1980; Isern, Labay & Canal 1984) and that some stellar collapses produce a gaseous supernova remnant but not a neutron star.

Taking the beaming factor into account, the total number of active pulsars (with $L>0.3$ mJy kpc^2) in the Galaxy is about 2×10^5 with an uncertainty of about a factor of 2. The total number of pulsars born in the Galaxy, assuming a galactic age of 12×10^9 yr and a constant birthrate, is between 10^8 and 4×10^8, so only about 0.1 per cent of the pulsars born are still active. The inactive pulsars will form a halo population, because of their high average velocity; the total mass will be a fraction of one per cent of the total galactic mass. Because of its relatively low mass, the pulsar component is unlikely to have a significant effect on the dynamics of the Galaxy.

With the recent discovery of two pulsars with millisecond periods (Backer *et al.* 1982; Boriakoff, Buccheri & Fauci 1983), it has become clear that observational knowledge of the short-period end of the pulsar period distribution is inadequate. There may be a second class of pulsars that are formed through a different evolutionary process with smaller magnetic fields and larger angular momenta than the typical 'slow' pulsars. It is too soon to tell whether fast pulsars will have a significant impact on the birthrate question, but our present inclination is that they are likely to be, at most, a 10 per cent perturbation on the total population.

References

Ables, J. G. & Manchester, R. N., 1976. *Astr. Astrophys.*, **50,** 177.
Anderson, B. & Lyne, A. G., 1983. *Nature,* **303,** 597.
Anderson, B., Lyne, A. G. & Peckham, R. J., 1975. *Nature,* **258,** 215.
Armstrong, J. W., Cordes, J. M. & Rickett, B. J., 1981. *Nature,* **291,** 561.
Arnaud, M. & Rothenflug, R., 1980. *Astr. Astrophys.*, **87,** 196.
Arnett, W. D. & Lerche, I., 1981. *Astr. Astrophys.*, **95,** 308.
Ashworth, M. & Lyne, A. G., 1981. *Mon. Not. R. astr. Soc.*, **195,** 517.

Backer, D. C. & Sramek, R. A., 1981. *Pulsars, IAU Symp. No. 95,* p.205, eds Sieber, W. & Wielebinski, R. Reidel, Dordrecht, Holland.
Backer, D. C., Kulkarni, S. R., Heiles, C., Davis, M. M. & Goss, W. M., 1982. *Nature,* **300,** 615.
Backus, P. R., Taylor, J. H. & Damashek, M. 1982. *Astrophys. J.,* **255,** L63.
Booth, R. S. & Lyne, A. G., 1976. *Mon. Not. R. astr. Soc.,* **174,** 53P.
Boriakoff, V. Buccheri, R. & Fauci, F., 1983. *Nature,* **304,** 417.
Caswell, J. L. & Lerche, I., 1979. *Mon. Not. R. astr. Soc.,* **187,** 201.
Caswell, J. L., Roger, R.S., Murray, J. D., Cole, D. J. & Cooke, D. J., 1975. *Astr. Astrophys.,* **45,** 239.
Clark, D. H. & Caswell, J. L., 1976. *Mon. Not. R. astr. Soc.,* **174,** 267.
Clark, D. H. & Stephenson, F. R., 1977. *Mon. Not. R. astr. Soc.,* **179,** 87P.
Cox, D. P. & Anderson, P. R., 1982. *Astrophys. J.,* **253,** 268.
Damashek, M., Backus, P. R., Taylor, J. H. & Burkhardt, R. K., 1982. *Astrophys. J.,* **253,** L57.
Damashek, M. Taylor, J. H. & Hulse, R. A., 1978. *Astrophys. J.,* **225,** L31.
Davies, J. G., Lyne, A. G. & Seiradakis, J. H., 1972. *Nature,* **240,** 229.
Davies, J. G., Lyne, A. G. & Seiradakis, J. H., 1973. *Nature Phys. Sci.,* **244,** 84.
Davies, J. G., Lyne, A. G. & Seiradakis, J. H., 1977. *Mon. Not. R. astr. Soc.,* **179,** 635.
Dewey, R. J., 1984. *PhD thesis,* Princeton University.
Fujimura, F. S. & Kennel, C. F., 1980. *Astrophys. J.,* **236,** 245.
Gailly, J. L., Lequeux, J. & Masnou, J. L., 1978. *Astr. Astrophys.,* **70,** L15.
Georgelin, Y. M. & Georgelin, Y. P., 1976. *Astr. Astrophys.,* **49,** 57.
Gomez-Gonzalez, J. & Guelin, M., 1974. *Astr. Astrophys.,* **32,** 441.
Gordon, K. J. & Gordon, C. P., 1975. *Astr. Astrophys.,* **40,** 27.
Graham, D. A., Mebold, U., Hesse, K. H., Hills, D. L. & Wielebinski, R., 1974. *Astr. Astrophys.,* **37,** 405.
Gullahorn, G. E. & Rankin, J. M., 1978. *Astr. J.,* **83,** 1219.
Gunn, J. E. & Ostriker, J. P., 1970. *Astrophys. J.,* **160,** 979.
Guseinov, O. Kh., Kasumov, F. K. & Yusifov, I. M., 1982a. *Soviet Astr.,* **25,** 567.
Guseinov, O. Kh., Kasumov, F. K. & Yusifov, I. M., 1982b. *Soviet Astr.,* **26,** 31.
Gwinn, C. R., 1984. *PhD thesis,* Princeton University.
Hall, A. N., 1980. *Mon. Not. R. astr. Soc.,* **191,** 751.
Harding, D. S. & Harding, A. K., 1982. *Astrophys. J.,* **257,** 603.
Haslam, C. G., Salter, C. J., Stoffel, H. & Wilson, W. E., 1982. *Astr. Astrophys. Suppl.,* **47,** 1.
Helfand, D. J. & Tademaru, E., 1977. *Astrophys. J.,* **216,** 842.
Higdon, J. C. & Lingenfelter, R. E., 1980. *Astrophys. J.,* **239,** 867.
Hillebrandt, W., 1982. In: *Supernovae: A survey of Current Research,* p. 123, eds Rees, M. J. & Stoneham, R. J., Reidel, Dordrecht, Holland.
Hillebrandt, W., Nomoto, K. & Wolff, R. G., 1984. *Astr. Astrophys.,* **133,** 175.
Huang, K.-l., Peng, Q.-h., He, X.-t. & Tong, Y., 1980. *Acta Astr. Sinica,* **21,** 237.
Hulse, R. A. & Taylor, J. H., 1974. *Astrophys. J.,* **191,** L59.
Hulse, R. A. & Taylor, J. H., 1975. *Astrophys. J.,* **201,** L55.
Isern, J., Labay, J. & Canal, R., 1984. *Nature,* **309,** 431.
Kafatos, M., Sofia, S., Bruhweiler, F. & Gull, T., 1980. *Astrophys. J.,* **242,** 294.
Large, M. I., 1971. *The Crab Nebula, IAU Symp. No. 46,* p. 165, eds Davies, R. D. & Smith, F. G., Reidel, Dordrecht, Holland.
Lyne, A. G., 1981. *Pulsars, IAU Symp. No. 95,* p. 423, eds Sieber, W. & Wielebinski, R., Reidel, Dordrecht, Holland.
Lyne, A. G., Anderson, B. & Salter, M. J., 1982. *Mon. Not. R. astr. Soc.,* **201,** 503.
Lyne, A. G., Ritchings, R. T. & Smith, F. G., 1975. *Mon. Not. R. astr. Soc.,* **171,** 579.
Manchester, R. N. & Peters, W. L., 1972. *Astrophys. J.,* **173,** 221.
Manchester, R. N. & Taylor, J. H., 1977. *Pulsars,* W. H. Freeman, San Francisco.
Manchester, R. N. & Taylor, J. H., 1981. *Astr. J.,* **86,** 1953.
Manchester, R. N., D'Amico, N. & Tuohy, I. R., 1985. *Mon. Not. R. astr. Soc.,* **212,** 975.
Manchester, R. N., Lyne, A. G., Taylor, J. H., Durdin, J. M., Large, M. I. & Little, A. G., 1978. *Mon. Not. R. astr. Soc.,* **185,** 409.
Manchester, R. N., Taylor, J. H. & Van, Y. Y., 1974. Astrophys. J., **189,** L119.
Manchester, R. N., Tuohy, I. R. & D'Amico, N., 1982. *Astrophys. J.,* **262,** L31.
Manchester, R. N., Wellington, K. J. & McCulloch, P. M., 1981. *Pulsars, IAU Symp. No. 95,* p. 445, eds Sieber, W. & Wielebinski, R., Reidel, Dordrecht, Holland.
Miller, G. E. & Scalo, J. M., 1979. *Astrophys. J. Suppl.,* **41,** 513

Mills, B., 1983. *Supernova Remnants and their X-ray Emission, IAU Symp. No. 101,* p. 551, eds Danziger, J., & Gorenstein, P., Reidel, Dordrecht, Holland.
Morini, M., 1981. *Astr. Astrophys.,* **104,** 75.
Narayan, R. & Vivekanand, M., 1983. *Astr. Astrophys.,* **122,** 45.
Newton, L. M., Manchester, R. N. & Cooke, D. J., 1981. *Mon. Not. R. astr. Soc.,* **194,** 841.
Nomoto, K., 1980. *Space Sci. Rev.,* **27,** 563.
Nomoto, K., 1984. *Astrophys. J.,* **277,** 791.
Ostriker, J. P. & Gunn, J. E., 1969. *Astrophys. J.,* **157,** 1395.
Pacini, F., 1967. *Nature,* **216,** 567.
Pacini, F., 1968. *Nature,* **221,** 454.
Phinney, E. S. & Blandford, R. D., 1981. *Mon. Not. R. astr. Soc.,* **194,** 137.
Prentice, A. J. R. & ter Haar, D., 1969. *Mon. Not. R. astr. Soc.,* **146,** 423.
Reimers, D. & Koester, D., 1982. *Astr. Astrophys.,* **116,** 341.
Richstone, D. O. & Davidson, K., 1972. *Astr. J.,* **77,** 198.
Ritchings, R. T., 1976. *Mon. Not. R. astr. Soc.,* **176,** 249.
Robinson, B. J., Manchester, R. N., Whiteoak, J. B., Sanders, D. B., Scoville, N. & Solomon, P. M., 1984. *Astrophys. J.,* in press.
Salter, M. J., Lyne, A. G. & Anderson, B., 1979. *Nature,* **280,** 477.
Sivan, J. P., 1974. *Astr. Astrophys.,* **16,** 163.
Srinivasan, G., & Dwarakanath, K. S., 1982. *J. Astrophys. Astr.,* **3,** 351.
Tammann, G. A., 1982. In: *Supernovae: A survey of Current Research,* p. 371, eds Rees, M. J. & Stoneham, R. J., Reidel, Dordrecht, Holland.
Taylor, J. H. & Manchester, R. N., 1977. *Astrophys. J.,* **215,** 885.
Taylor, J. H., Gwinn, C. R., Weisberg, J. M. & Rawley, L. A., 1984. *Very Long Baseline Interferometry, IAU Symp. No. 110,* ed. Setti, G., Reidel, Dordrecht, Holland (in press).
Vivekanand, M. & Narayan, R., 1981. *J. Astrophys. Astr.,* **2,** 315.
Vivekanand, M. & Narayan, R., 1982. *J. Astrophys. Astr.,* **3,** 237.
Vivekanand, M., Narayan, R. & Radhakrishnan, V., 1982. *J. Astrophys. Astr.,* **3,** 237.
Wood, P. R., Bessell, M. S. & Fox, M. W., 1983. *Astrophys. J.,* **272,** 9.

Appendix A

The sensitivity of pulsar surveys is known to be reduced for short-period pulsars owing to dilution of the pulses from instrumental effects, from dispersion smearing in the receiver passband, and from scattering in the interstellar medium. In existing surveys the last two effects probably affect only a minority of distant and therefore high-luminosity pulsars. The main instrumental effect is the post-detection integration time, the result of which can be quantified statistically. For most of the large-scale pulsar surveys completed to date, the integration time is equivalent to a convolution of the data with a smoothing function of $t_i \approx 0.02$ s duration. If a pulsar has a pulse of intrinsic width w, then the observed width is increased to approximately

$$w_e=(w^2+t_i^2)^{1/2} \tag{A.1}$$

and the sensitivity of the search will be reduced by a factor

$$f=(w_e/w)^{1/2}=(1+t_i^2/w^2)^{1/4}. \tag{A.2}$$

For an infinite planar galaxy the number of such pulsars detected will be reduced by this same factor.

Pulsars have a duty cycle w/P which (with a few exceptions) is independent of period P and about equal to 0.04. Therefore, on average, pulsars of period P will be undercounted in the surveys by the factor

$$f=\left[1+\left(\frac{t_i}{0.04\,P}\right)^2\right]^{1/4}=\left[1+\left(\frac{0.5}{P}\right)^2\right]^{1/4}. \tag{A.3}$$

In Fig. 11 the broken-line histogram is the observed period distribution, and the full-line histogram is the period distribution corrected by this factor.

Appendix B

A Monte Carlo technique was used to estimate the function $V(R, z, L)$ which represents the volume of the Galaxy effectively surveyed for pulsars of luminosity L at distance R from the galactic centre and z from the galactic plane. As described in Section 3, a grid was defined consisting of 20 concentric 1-kpc rings in R, 30 horizontal 0.1-kpc slices in z, and 15 semi-decade intervals of L covering the range $0.03<L<10^6$ mJy kpc^2. A large number ($\sim 10^5$) of potential pulsar locations (R, θ, z) were then chosen at random within the spatial grid. For each position we computed the galactic coordinates l and b, the distance d from the Sun, and the dispersion measure DM corresponding to our model of the galactic electron density distribution, equation (2.1). For each pulsar survey that searched the direction (l, b), the minimum detectable flux density $S_{\min}$ was estimated. The smallest of these values determined the minimum luminosity for a detectable pulsar at that position, according to the relation

$$L_0 = S_{\min} d^2. \tag{B.1}$$

All cells of the array V at $(R, z, L \geq L_0)$ were then incremented by appropriate amounts, and the process was repeated.

The crucial part of the calculation is finding the minimum detectable flux density, $S_{\min}$. For this purpose we have used the basic relation

$$S_{\min} = \beta S_0 g(T_{\rm sky}) h(DM), \tag{B.2}$$

where β is a factor (generally between 1 and 2) that represents statistically the degradation of sensitivity for pulsars not located exactly at the beam-centre directions covered by the survey; S_0 is the nominal minimum detectable flux density for a particular survey; $g(T_{\rm sky})$ gives the functional dependence of sensitivity on sky background temperature $T_{\rm sky}(l, b)$; and $h(DM)$ gives the dependence of sensitivity on dispersion measure. The equations used were as follows, with $S_{\min}$ in units of mJy, $T_{\rm sky}$ in kelvin, and DM in cm^{-3} pc.

Jodrell Bank survey (Davies *et al.* 1972, 1973):

$$S_{\min} = 12\beta \left[\frac{110 + T_{\rm sky}}{140}\right]\left[1 + \left(\frac{DM}{180}\right)^2\right]^{1/4}. \tag{B.3}$$

UMass–Arecibo survey (Hulse & Taylor 1974, 1975):

$$S_{\min} = 1.5\beta \left[\frac{110 + T_{\rm sky}}{260}\right], \quad DM < 640, \tag{B4a}$$

$$S_{\min} = 2.1\beta \left[\frac{110 + T_{\rm sky}}{260}\right], \quad DM > 640. \tag{B.4b}$$

Second Molonglo survey (Manchester *et al.* 1978):

$$S_{\min} = 8\beta \left[\frac{210 + T_{\rm sky}}{240}\right]\left[1 + \left(\frac{DM}{70}\right)^2\right]^{1/4}, \quad b > 18°, \tag{B.5a}$$

$$S_{\min} = 9\beta \left[\frac{210 + T_{\rm sky}}{240}\right], \quad b < 18°, \quad DM < DM_0, \tag{B.5b}$$

$$S_{\min} = 9\beta \left[\frac{210 + T_{\rm sky}}{240}\right]\left[1 + \left(\frac{DM - DM_0}{70}\right)^2\right]^{1/4}, \quad b < 18°, \quad DM > DM_0. \tag{B.5c}$$

UMass–NRAO survey (Damashek *et al.* 1978, 1982):

$$S_{\min}=10\beta\left[\frac{170+T_{\rm sky}}{200}\right], \quad DM<120, \tag{B.6a}$$

$$S_{\min}=10\beta\left[\frac{170+T_{\rm sky}}{200}\right]\left[1+\left(\frac{DM-120}{16}\right)^2\right]^{1/4}, \quad DM>120. \tag{B.6b}$$

In equations (B.5b) and (B.5c), the parameter DM_0 is equal to $130\,n$, where $n=6.6/\sin|b|$ is the integral number of dispersion channels (between 1 and 6) that were searched.

The various constants and parameters in equations (B.3) through (B.6) depend on details of the antennas, receivers, and analysis techniques used in the four surveys, further information on which can be found in the original references. The sky background temperatures were taken from a machine-readable version of the 408-MHz all-sky map by Haslam *et al.* (1982).